Advances in Science and Technology Research Journal

Advances in Science and Technology Research Journal, 2026, 20(9), 270–285
https://doi.org/10.12913/22998624/224180
ISSN 2299-8624, License CC-BY 4.0

Received: 2026.05.12
Accepted: 2026.07.10
Published: 2026.08.01

Analysis of adsorption equilibria and surface energetic properties of stationary phases in selected hydrophilic interaction liquid chromatography systems

Regina Lech-Przywara[1*], Weronika Sofińska-Chmiel[2], Mateusz Przywara[3], Wojciech Zapała[3]

[1] Doctoral School of the Rzeszow University of Technology, ul. Akademicka 2, 35-084 Rzeszów, Poland
[2] Analytical Laboratory, Institute of Chemical Sciences, Faculty of Chemistry, Maria Curie-Skłodowska University in Lublin, plac Maria Curie-Skłodowska 3, 20-031 Lublin, Poland
[3] Department of Chemical and Process Engineering, Faculty of Chemistry, Rzeszow University of Technology, Al. Powstańców Warszawy 6, 35-959 Rzeszów, Poland
* Corresponding author's e-mail: d555@stud.prz.edu.pl, ichwz@prz.edu.pl

ABSTRACT

This study focused on the analysis of adsorption equilibria of phenol and caffeine using two chromatographic columns employed in hydrophilic interaction liquid chromatography (HILIC): Hypersil GOLD HILIC and Shodex SILICA 5NH 4D. The aim of the study was to determine the energetic properties of the surfaces of the tested adsorbents depending on the composition of the mobile phase and in systems with two chemically different analytes. Adsorption isotherms were determined experimentally in systems with mobile phases of varying proportions of acetonitrile and methanol. The obtained equilibrium data were first analyzed using Scatchard plots, and in the in the subsequent step, the adsorption energy distribution was determined using the EM (expectation–maximization) method. In both columns, low-energy adsorption sites play a dominant role. However, under specific chromatographic conditions, the involvement of high-energy adsorption sites is also observed, indicating the heterogeneous nature of the stationary phase surfaces. The results enabled the selection of the most appropriate adsorption isotherm model and confirm that its proper choice is crucial for the correct interpretation of adsorption equilibrium data in HILIC systems. At the same time, they highlight the importance of accounting for surface heterogeneity in the development and optimization of chromatographic methods.

Keywords: adsorption energy distribution, adsorption isotherm, frontal analysis, HILIC, isotherm model, liquid chromatography, stationary phase.

INTRODUCTION

The retention mechanism in liquid chromatography is not yet fully understood and remains the subject of investigation by many research groups. This highlights the need for further studies, particularly in the case of HILIC chromatography, where the available scientific literature provides limited information on the influence of the surface energy state on the adsorption/retention mechanism. From this perspective, the present work aimed to bridge this gap, which constitutes both the novelty and the main objective of this study. In liquid chromatography, analytes can interact with the stationary phase through various mechanisms, which are characterized by different interaction energies. In addition, the surface of the stationary phase may exhibit energetic heterogeneity, resulting in different binding affinities of analyte molecules depending on the type of available interaction sites [1,2]. This heterogeneity arises from multiple factors, such as the chemical heterogeneity of the surface, the presence of functional groups with varying physicochemical properties and polarity, and the degree of surface modification. For silica-based phases, silanol

groups play a particularly important role, as they can participate in strong interactions, especially with polar and ionic analytes. In addition, surface heterogeneity is influenced by the porous structure of the adsorbent and the presence of trace metallic impurities (e.g., Fe, Ni), which modify the local energetic properties of the surface [3–5]. Energetic heterogeneity of the stationary phase surface significantly affects chromatographic separation. The molecules that are more strongly bound to high-energy adsorption sites undergo slower desorption, leading to peak asymmetry in chromatography, most commonly observed as peak tailing. This results in reduced column efficiency and poorer chromatographic resolution. Another consequence of surface heterogeneity is a decrease in the effective adsorption capacity, since the highest-energy sites are occupied first, which may reduce method sensitivity, particularly in trace analysis [2,6–8]. Analysis of the adsorption energy distribution (AED) provides a useful approach to describing the adsorption process, as it enables the determination of the number of available active sites and the characteristic adsorption energies associated with them [2,7,9–11]. AED provides detailed information on the energy distribution of adsorption sites, allowing for the characterization of adsorption heterogeneity. The total amount of adsorbed substance is determined by integrating the contributions of all adsorption sites over a specified energy range [ε_{max}, ε_{min}], where ε_{max} and ε_{min} denote the maximum and minimum adsorption energy, respectively (Equation 1) [2,7].

$$q(C) = \int_{\varepsilon_{min}}^{\varepsilon_{max}} f(\varepsilon) \cdot \theta(C, \varepsilon) d\varepsilon \qquad (1)$$

where: $q(C)$ is the experimentally determined adsorption isotherm, $f(\varepsilon)$ is the distribution of adsorption energies, ε is the adsorption energy (i.e., the binding energy of the adsorbate to a specific active site), and $\theta(C, \varepsilon)$ represents the local adsorption model describing sites with adsorption energy ε [2,7].

Several numerical methods are used for the analysis of the adsorption energy distribution. In chromatographic data analysis, the expectation–maximization (EM) algorithm (Equation 2) is frequently employed, which allows for the determination of adsorption equilibrium constant distributions without assuming a specific energy distribution model. The algorithm operates iteratively by alternately performing the expectation (E) and maximization (M) steps until convergence is achieved [2,7,11–14].

$$q_{calc}(C_j) = \sum_{i=1}^{p} f(ln\, K_i) \cdot \theta(C_j, K_i) \Delta \ln K \qquad (2)$$

where: $q_{calc}(C_j)$ is the calculated amount of adsorbed substance for the j-th point of the isotherm, $f(ln\ K_i)$ denotes the value of the distribution function of adsorption equilibrium constants at the point corresponding to K_i and $\theta(C_j, K_i)$ represents the local degree of coverage of adsorption sites with energy corresponding to K_i at the analyte concentration C_j.

The *ln K* domain is divided into a uniform grid consisting of p points, and the distance between adjacent grid points is equal to $\Delta ln\, K$. In this study, the adsorption energy scale is expressed in terms of *ln K*, which is proportional to the change in the Gibbs free energy of adsorption [2,7,11–14].

The energetic heterogeneity of the stationary phase surface is particularly important in hydrophilic interaction liquid chromatography (HILIC), used for the separation of highly polar compounds. In HILIC systems, the retention mechanism is complex and involves the simultaneous contribution of adsorption, partitioning between phases, electrostatic interactions, and hydrogen bonding [15–17]. An additional factor influencing the adsorption process is the presence of a thin layer of water adsorbed on the surface of the polar stationary phase, the properties of which depend on the composition of the mobile phase [18]. Due to the chemical and energetic heterogeneity of stationary phase surfaces used in HILIC systems, classical adsorption models assuming surface homogeneity, such as the Langmuir isotherm, do not always accurately describe the adsorption process. In such cases, analysis of the adsorption energy distribution (AED) is particularly useful, as it enables the quantitative characterization of adsorption sites with varying energies [19–21]. Therefore, in the present study, AEDs were determined to assess the degree of energetic heterogeneity of HILIC stationary phase surfaces, and the accuracy of selected adsorption isotherm models was subsequently compared: the

Langmuir model (Equation 3) for energetically homogeneous adsorbent surfaces, as well as the Tóth (Equation 4) and bi-Langmuir (Equation 5) models for energetically heterogeneous adsorbent surfaces. The mathematical forms of these models are given below and a detailed description is available in the literature [19–22].

$$q(C) = \frac{q_S K C}{1 + KC} \tag{3}$$

$$q(C) = \frac{q_S K C}{(1 + (KC)^{\nu})^{1/\nu}} \tag{4}$$

$$q(C) = \frac{q_{S1} K_1 C}{1 + K_1 C} + \frac{q_{S2} K_2 C}{1 + K_2 C} \tag{5}$$

where: $q(C)$ is the equilibrium analyte concentration in the stationary phase (g/L_{ads}), C is the analyte concentration in the mobile phase (g/L), q_s is the maximum adsorption capacity (g/L_{ads}), K is the adsorption equilibrium constant (L/g), q_{s1} and q_{s2} are the saturation capacities of adsorption sites (g/L_{ads}), K_1 and K_2 are the adsorption equilibrium constants corresponding to two types of adsorption sites (L/g) and ν is the heterogeneity parameter in the Tóth isotherm [19–22].

Such an approach enables not only the fitting of adsorption models to experimental data, but also the interpretation of the retention mechanism and the evaluation of the influence of the energetic characteristics of the stationary phase surface on the quality and efficiency of separation in HILIC systems.

MATERIALS AND METHODS

Materials

Phenol (PH) and caffeine (CAF), obtained from Merck, were selected as model compounds due to their different chemical properties, which enable a broad evaluation of the chromatographic system, particularly the stationary and mobile phases. Phenol, as a compound of moderate polarity, is suitable for studying interactions between the mobile and stationary phases, particularly under conditions where both hydrophobic and polar interactions play a significant role. Caffeine, which is more polar than phenol, enables the investigation of the behavior of the chromatographic system toward compounds that interact more strongly with the eluent [14]. The use of two analytes with different physicochemical properties enables the evaluation of the influence of their characteristics on the adsorption process, as well as the manner in which the heterogeneity of the stationary phase surface manifests itself in the investigated chromatographic systems, thereby allowing for a better understanding of the adsorption mechanism and its dependence on chromatographic conditions. Methanol (MeOH) and acetonitrile (ACN), obtained from Merck, were used for the preparation of the mobile phases. Distilled, deionized, and demineralized water was obtained using a SolPure78Z deionizer (ELKAR). The solvent mixtures were degassed immediately after preparation using an ultrasonic bath (ULTRON) for 5 minutes. The studies were carried out using MeOH–water and ACN–water systems, with the volumetric fraction of the organic component set at 70% and 95% (v/v) in both systems.

Columns and instrumentations

Two chromatographic columns were used in the study, and their characteristics of which are shown in Table 1. It should be noted that both columns can be used in reversed-phase (RP), normal-phase (NP), and HILIC systems. Chromatographic analysis was carried out using a LaChrom system from Merck–Hitachi, equipped with an L-7100 pump, an L-7360 column thermostat, an L-7455 UV detector, an L-7612 degasser, and a D-7000 interface.

Methodology of study

Adsorption equilibrium – frontal analysis

The adsorption isotherms were determined using the well-established frontal analysis method. A detailed description of this method can be found in the literature, e.g., [21–25].

The concentrations of the test solutions were as follows: for PH: 1; 6; 10; 20; 30; 40; 50; 60; 70; 80; 90; 100; and 120 g/L, whereas for CAF: 0.1; 0.5; 0.8; 1; 2; 3.5; 5; 6.75; 8.25; 10.5; 12; 13.5; and 15 g/L. The measurements were performed at 20 °C and with a mobile phase flow rate of 1 mL/min. Before starting each series of experiments, each column was stabilized by flushing it

Table 1. Chromatographic column parameters

Chromatographic column name	Hypersil GOLD HILIC	Shodex SILICA 5NH 4D
Diameter (metric) (mm)	4.6	4.6
Length (metric) (mm)	150	150
Max. pressure (bar)	400	200
Particle size (µm)	5	5
Pore size (Å)	175	100
Stationary phase	Polar silica	Aminopropyl

with the mobile phase in an amount corresponding to twenty column volumes (as recommended by the manufacturer). Detection was performed at wavelengths of 250 nm for CAF and 270 nm for PH. The sample volume injected into the column was 5 mL. The measurements were repeated three times, and good repeatability of the results was achieved (the differences were statistically insignificant). Based on the obtained breakthrough curves for individual concentrations, experimental adsorption isotherms were determined using calibration curves describing the relationship between detector signal and concentration. Subsequently, to determine the adsorption energy distribution (AED), a computational program developed by Stanley et al. [2], based on the EM algorithm, was used. The input data for the calculations included the experimental adsorption isotherm, the minimum and maximum values of the adsorption equilibrium constant determined from the extreme analyte concentrations obtained in frontal analysis, and the number of points (p) in the energy grid. Based on the obtained isotherms, adsorption energy distributions, and Scatchard plots, a preliminary selection of the isotherm model was performed. Subsequently, using OriginPro 8.5.1, the model parameters were estimated by minimizing the sum of squared differences between experimental and theoretical values, employing the Levenberg–Marquardt algorithm. The following models were compared: Langmuir (denoted as M_1), Tóth (denoted as M_2), and bi-Langmuir (denoted as M_3) isotherms. The adequacy of model fitting was evaluated using Fisher's test (F), which served as a statistical criterion for assessing the quality of the fit to the experimental data, as well as by means of the sum of squared residuals (RSS) and the standard deviation (SD). The analyzed adsorption isotherm models were also compared based on the ratio of Fisher test values for pairs of models. For two adsorption isotherm models M_i and M_j, the ratio of the Fisher tests, F_{M_i, M_j} was calculated according to the following relationship (Equation 6) [26]:

$$F_{M_i,M_j} = \frac{F_{M_i}}{F_{M_j}} \tag{6}$$

where: F_{M_i, M_j} are the ratio of the Fisher's test values for models M_i and M_j, and F_{M_i} and $F_{M_{ij}}$ are the values of the Fisher's test for models M_i and M_j, respectively.

The use of the ratio of Fisher test values enables direct comparison of the goodness-of-fit of different models while simultaneously taking into account the number of estimated parameters, which is particularly important when analyzing models of varying complexity.

Considering the significance level α model M_i will describe the experimental data better than model M_j (i.e., it will be statistically superior) if the following relationship (Equation 7) is satisfied (i.e., is statistically true):

$$F_{M_i,M_j} \geq F_{N-l_i, N-l_j, \alpha} \tag{7}$$

where: N is the number of experimental data points, l_i and l_j are the numbers of parameters estimated during the fitting procedure for models M_i and M_j, respectively, α is the significance level and F_{N-l_i}, $N-l_j$, α is the values obtained from statistical tables for the given α. The assumed significance level (risk) was set at α = 0.05 [26].

In the analysis, the number of experimental data points N and the number of parameters estimated for the individual models l_i and l_j were taken into account, which allowed the determination of the appropriate degrees of freedom for the Fisher test. The degrees of freedom are directly derived from the relationship $N–l$, enabling the proper evaluation of critical values and the correct interpretation of the statistical significance of

the obtained results. In this approach, the degrees of freedom of the Fisher test are directly determined by the number of experimental data points and the number of estimated parameters, which allows for the proper evaluation of the statistical significance of differences between the compared models. It should be noted that although criteria such as AIC and BIC are commonly used for model comparison, the approach based on the ratio of Fisher test values allows one to assess whether one model provides a significantly better description of the data than another, or whether the observed differences are minor and may result from random variability in the experimental data. Thus, this approach not only identifies the best-fitting model, but also enables evaluation of whether its advantage over other models is pronounced and statistically justified [26–27].

RESULTS AND DISCUSSION

Adsorption equilibrium analysis

For the Hypersil GOLD HILIC column, the analysis of adsorption isotherms and Scatchard plots is presented in Figure 1 (for PH) and Figure 3 (for CAF), while the AEDs are shown in Figure 2 (for PH), and Figure 4 (for CAF). The adsorption energy distributions were expressed as adsorption capacity contributions q_s as a function of *ln K*. The Scatchard plots are linear for most systems, except for PH in 95% (v/v) ACN and CAF in 70% (v/v) ACN, where nonlinear behavior is observed, indicating energetic heterogeneity of the stationary phase surface. The AED analysis revealed at least two energetic adsorption sites: a dominant low-energy site and a smaller high-energy site associated with specific interactions, such as hydrogen bonding or donor–acceptor interactions. The presence of these high-energy adsorption sites can be related to the interactions between silanol groups present on the surface of the stationary phase and analyte molecules. Silanol groups can participate in hydrogen bonding as well as electrostatic interactions, leading to the formation of sites with increased adsorption energy. The differences between PH and CAF arise from their physicochemical properties. Caffeine, being more polar and richer in hydrogen-bond acceptor sites, interacts more strongly with high-energy sites, as evidenced by a distinct peak at higher values of *ln K*. Phenol mainly adsorbs on

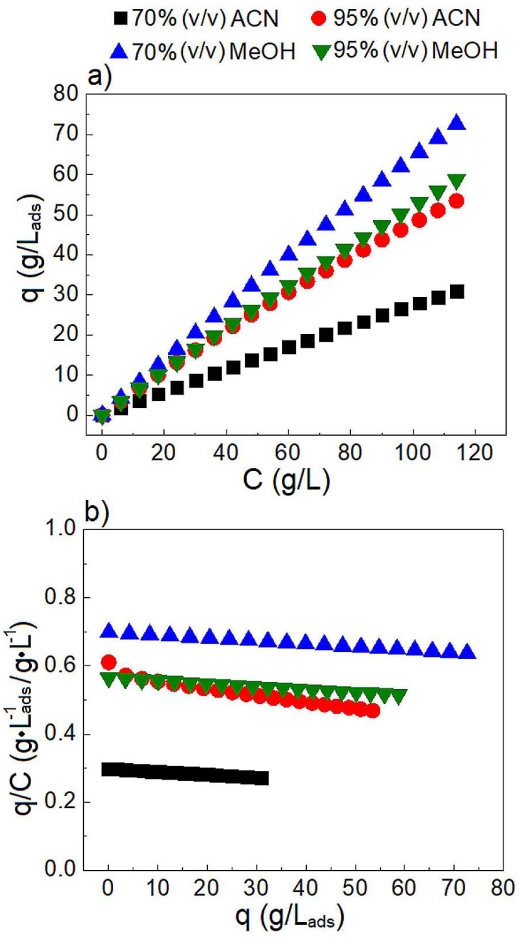

Figure 1. Experimentally determined: a) adsorption isotherms and b) Scatchard plots for PH in a Hypersil GOLD HILIC chromatographic column in different eluent compositions

low-energy sites. For CAF, the highest sorption capacity is observed in 95% (v/v) ACN, while the lowest occurs in 95% (v/v) MeOH, due to strong solvation in methanol rich mobile phases. Phenol shows greater sensitivity to mobile phase composition, with the highest sorption in 70% (v/v) MeOH and the lowest in 95% (v/v) ACN.

For the Shodex SILICA 5NH 4D column, adsorption studies of PH in 95% (v/v) ACN and 70% (v/v) MeOH showed a nonlinear Scatchard plot (Figure 5), indicating energetic heterogeneity of the stationary phase surface. This observation was confirmed by the AED analysis (Figure 6), which revealed an additional active site and a more complex retention mechanism than in the homogeneous model. Under the other conditions, i.e., 70% (v/v) ACN and 95% (v/v) MeOH, the Scatchard relationship (Figure 5) was linear, indicating surface homogeneity and the presence of a single adsorption site. The highest sorption

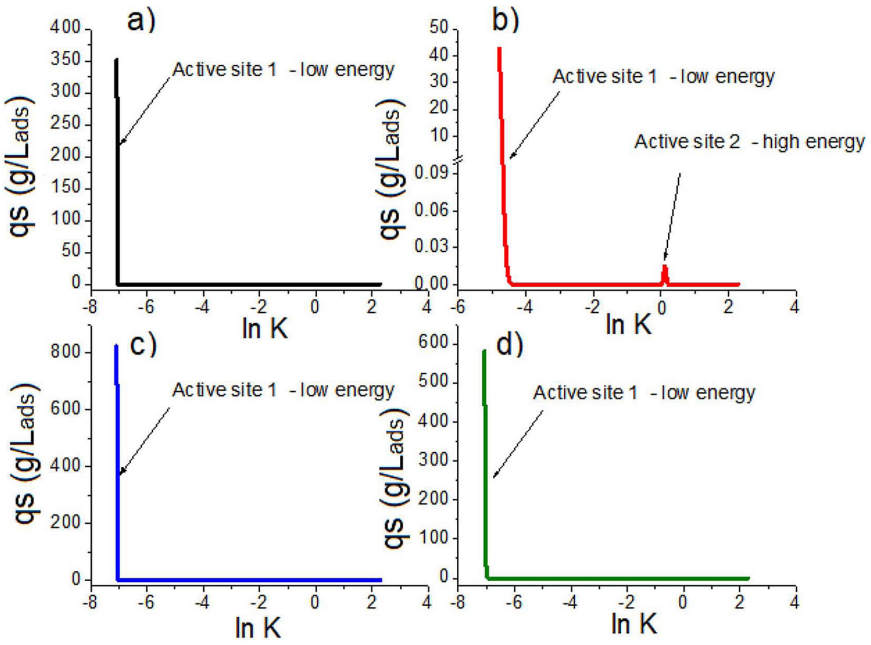

Figure 2. Adsorption energy distribution in a Hypersil GOLD HILIC column for PH in different eluent compositions: a) 70% (v/v) ACN, b) 95% (v/v) ACN, c) 70% (v/v) MeOH, d) 95% (v/v) MeOH

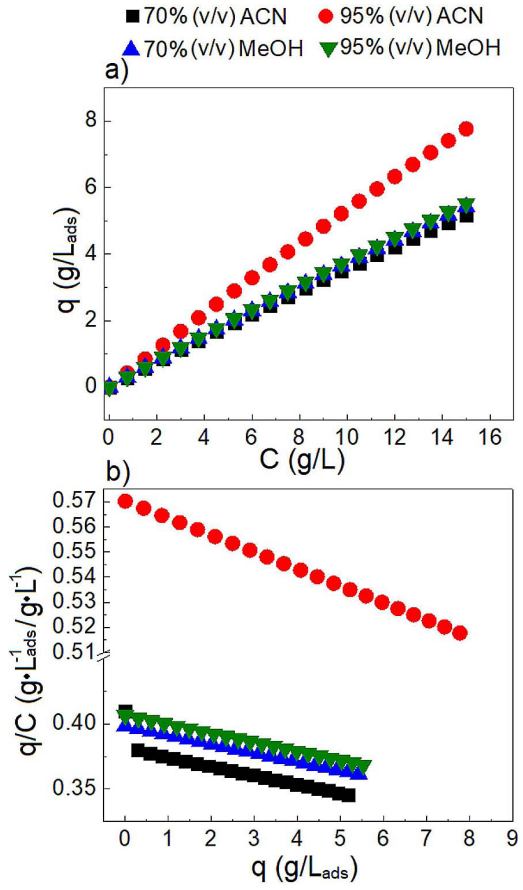

Figure 3. Experimentally determined: a) adsorption isotherms and b) Scatchard plots for CAF in a Hypersil GOLD HILIC chromatographic column in different eluent compositions

capacity of PH was observed in 95% (v/v) ACN, whereas the lowest was found in 70% (v/v) ACN. For CAF in systems containing 70% (v/v) ACN and 95% (v/v) ACN, a nonlinear Scatchard relationship (Figure 7) was observed, indicating the surface heterogeneity of the stationary phase. This was confirmed by AED analysis (Figure 8), which suggested the presence of more than one type of active site responsible for different interactions between CAF and the surface. In the case of CAF, which contains multiple functional groups capable of accepting hydrogen bonds, the interactions with aminopropyl groups may be stronger, promoting the formation of higher-energy adsorption sites and a more pronounced manifestation of surface heterogeneity. In the systems containing 70% (v/v) and 95% (v/v) MeOH, the Scatchard relationship (Figure 7) was linear, indicating surface homogeneity and a single type of adsorption site for CAF. The observed differences result from the influence of eluent composition on CAF solvation and the exposure of aminopropyl groups on the surface. In acetonitrile-containing systems, solvation of the polar part of the analyte is weakened, which enhances the interactions between CAF and the adsorbent and may reveal or activate higher energy binding sites. Under such conditions, reduced competition from solvent molecules favors direct analyte surface interactions, including hydrogen bonding and

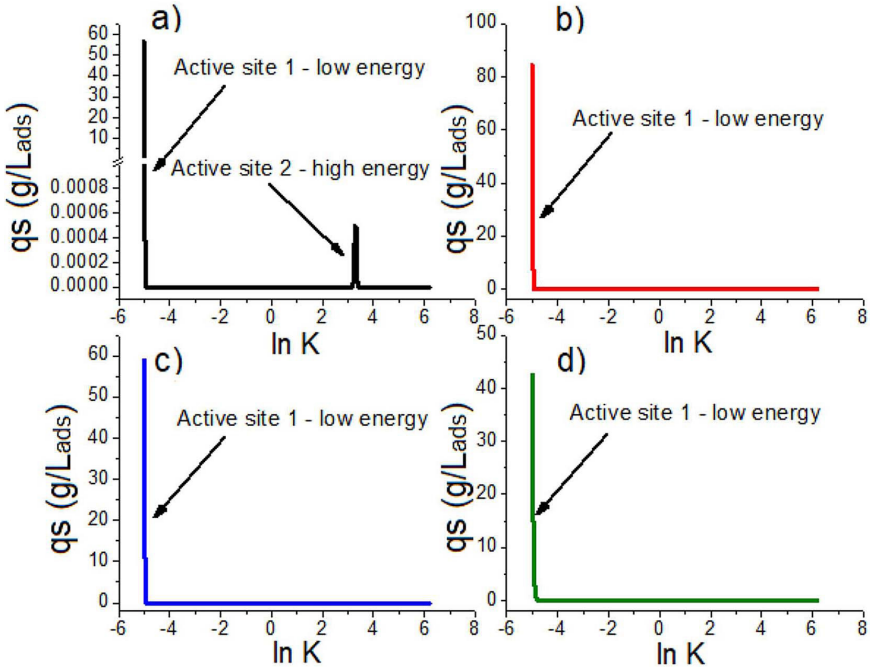

Figure 4. Adsorption energy distribution in a Hypersil GOLD HILIC column for CAF in different eluent compositions: a) 70% (v/v) ACN, b) 95% (v/v) ACN, c) 70% (v/v) MeOH, d) 95% (v/v) MeOH

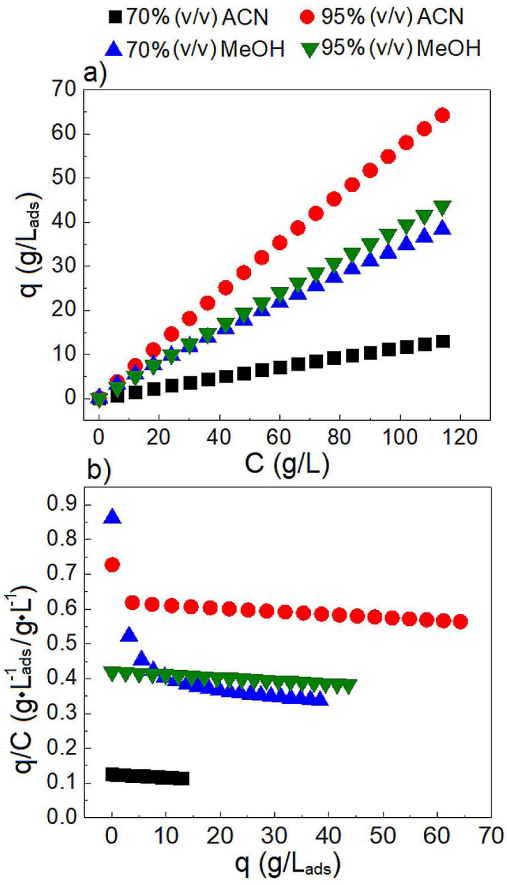

Figure 5. Experimentally determined: a) adsorption isotherms and b) Scatchard plots for PH in a Shodex SILICA 5NH 4D chromatographic column in different eluent compositions

donor–acceptor interactions. In methanol-based systems, solvation is stronger, making interactions with energetically heterogeneous adsorption sites less accessible. Methanol, as a protic solvent, may also compete with the analyte for active sites through hydrogen bonding with aminopropyl groups, leading to more homogeneous adsorption behavior. The highest sorption capacity of CAF was observed in 95% (v/v) ACN, whereas the lowest was found in 70% (v/v) ACN, where stronger solvation limits the number of accessible active sites.

Comparison of the accuracy of adsorption isotherm models

Experimentally obtained adsorption isotherms, together with Scatchard plots (Figures 1, 3, 5, 7) and the derived AEDs (Figures 2, 4, 6, 8), provide direct information for selecting an appropriate adsorption isotherm model. The selection of a suitable isotherm model is crucial for optimizing the separation process, which is typically performed numerically using models of column sorption dynamics. The observed nonlinearity of Scatchard plots and the presence of at least two distinct active sites in AED indicate that simple homogeneous models (e.g., the Langmuir isotherm) may not adequately describe the data. In practice, this implies that, when comparing

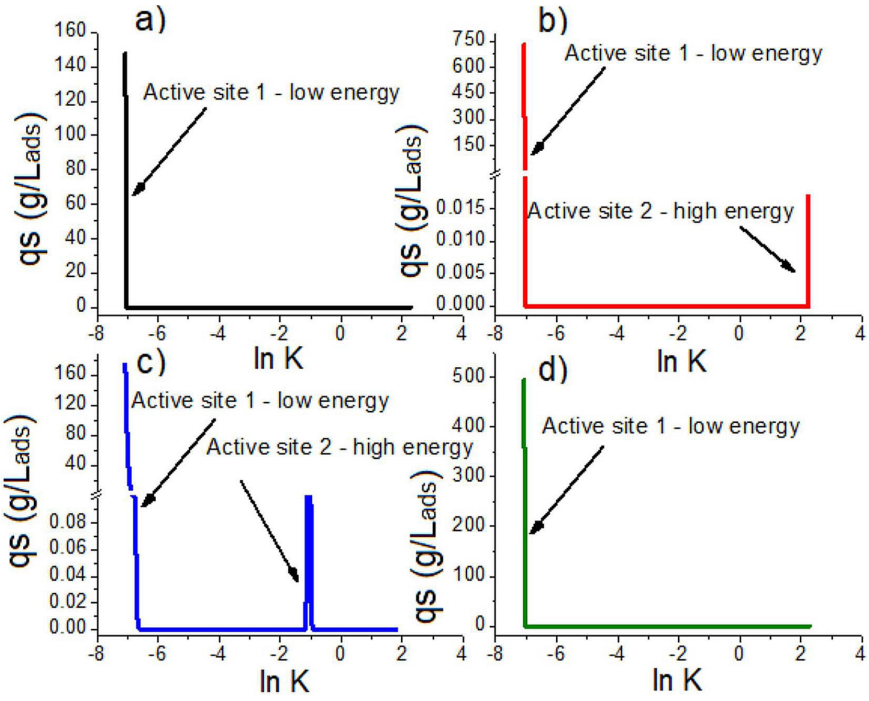

Figure 6. Adsorption energy distribution in a Shodex SILICA 5NH 4D column for PH in different eluent compositions: a) 70% (v/v) ACN, b) 95% (v/v) ACN, c) 70% (v/v) MeOH, d) 95% (v/v) MeOH

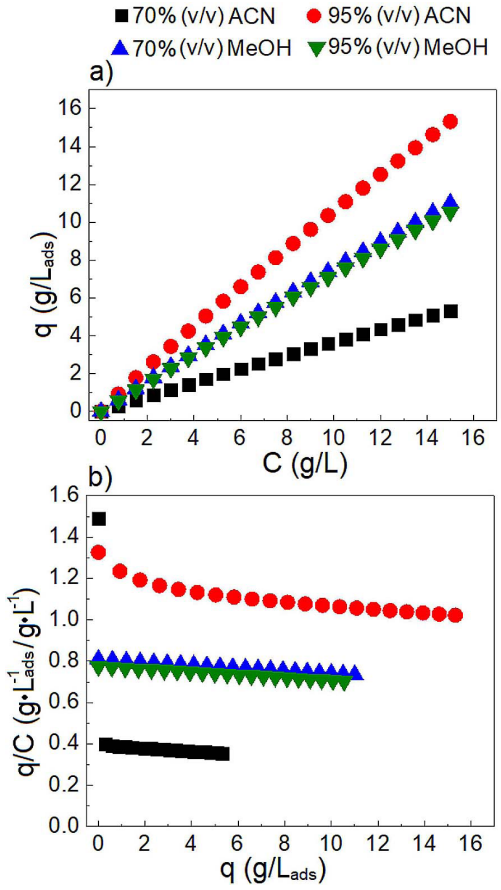

Figure 7. Experimentally determined: a) adsorption isotherms and b) Scatchard plots for CAF in a Shodex SILICA 5NH 4D chromatographic column in different eluent compositions

adsorption isotherm models, heterogeneous models (e.g., the bi-Langmuir isotherm) or generalized isotherms such as the Tóth model should be considered, as they account for the energetic heterogeneity of the stationary phase.

For the Hypersil GOLD HILIC column, the PH data in the 70% (v/v) ACN system as well as in the 70% and 95% (v/v) MeOH systems indicate surface homogeneity of the stationary phase, which justifies the application of the Langmuir model. The estimated parameters, q_s and K (Table 2) fall within the expected range, and the values of the parameter, v, in the Tóth model are close to 1, indicating the absence of significant surface heterogeneity. This is confirmed by statistical analysis (Table 3), which shows that the Langmuir model has lower RSS and SD values as well as higher F-test values than the other models. Different behavior is observed in the 95% (v/v) ACN system, for which energetic heterogeneity of the surface is observed. This is evidenced by a significant decrease in the value of the Tóth model parameter v (≈ 0.856) and a poorer fit of the Langmuir model (higher RSS and SD values, and a lower F-test value). In this case, a better fit was obtained for heterogeneous models. A comparison of the models with the help of the ratio of F-test values (Table 4) showed that, for the 95% (v/v) ACN system, the Tóth model describes the

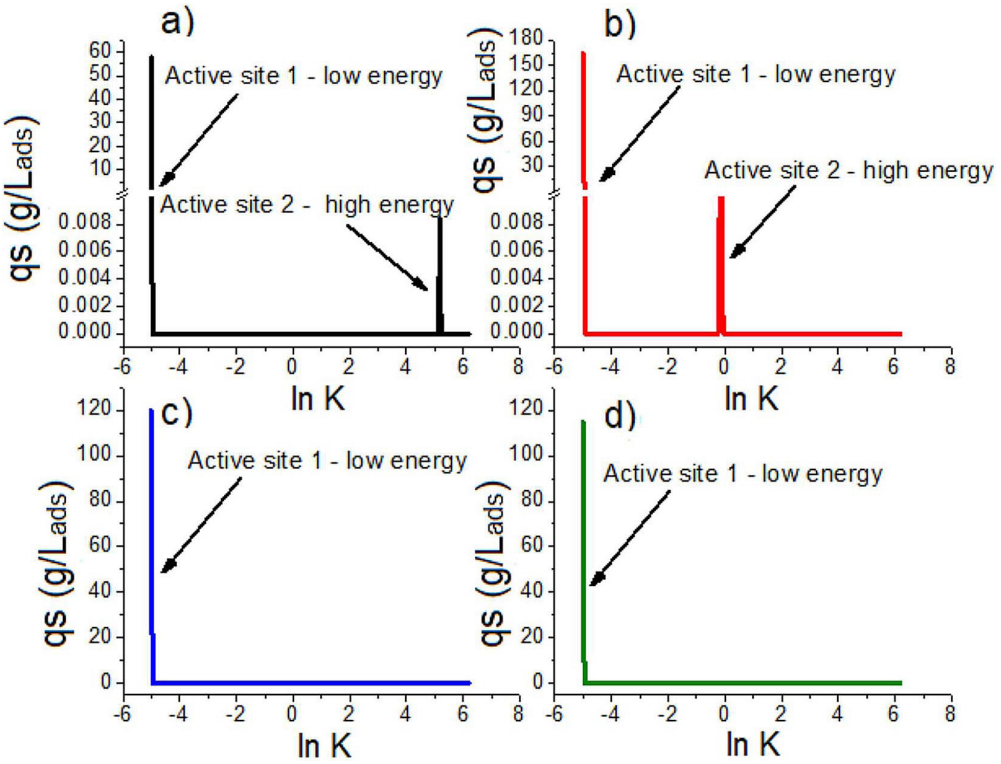

Figure 8. Adsorption energy distribution in a Shodex SILICA 5NH 4D column for CAF in different eluent compositions: a) 70% (v/v) ACN, b) 95% (v/v) ACN, c) 70% (v/v) MeOH, d) 95% (v/v) MeOH

Table 2. Estimated values of the adsorption isotherm model parameters along with confidence intervals for the Hypersil GOLD HILIC column

	ACN/MeOH content in the eluent % (v/v)		Langmuir isotherm (M_1)		Tóth isotherm (M_2)		
			K(L/g)	q_s(g/L_{ads})	K (L/g)	q_s (g/L_{ads})	v
PH	ACN	70	$8.49\times10^{-4} \pm 2.88\times10^{-9}$	$351.28 \pm 1.11\times10^{-3}$	$8.51\times10^{-4} \pm 1.4\times10^{-6}$	350.18 ± 0.587	$1.001 \pm 5.96\times10^{-4}$
		95	$1.91\times10^{-3} \pm 3.03\times10^{-5}$	298.72 ± 4.09	$1.36\times10^{-3} \pm 1.42\times10^{-5}$	427.173 ± 4.72	0.856 ± 0.0038
	MeOH	70	$8.49\times10^{-4} \pm 2.88\times10^{-9}$	$822.81 \pm 2.6\times10^{-3}$	$8.51\times10^{-4} \pm 1.5\times10^{-6}$	819.99 ± 1.49	$1.001 \pm 6.47\times10^{-4}$
		95	$8.53\times10^{-4} \pm 4.79\times10^{-9}$	$662.1 \pm 3.46\times10^{-3}$	$8.55\times10^{-4} \pm 1.14\times10^{-6}$	660.46 ± 0.897	$1.0008 \pm 4.83\times10^{-4}$
CAF	ACN	70	$7.69\times10^{-3} \pm 4.3\times10^{-4}$	50 ± 2.55	$6.4\times10^{-3} \pm 1.33\times10^{-4}$	59.64 ± 1.27	$0.97 \pm 7.3\times10^{-3}$
		95	$6.75\times10^{-3} \pm 3.31\times10^{-7}$	$84.46 \pm 3.84\times10^{-4}$	$1.86\times10^{-2} \pm 6.4\times10^{-3}$	30 ± 10.56	$1.001 \pm 3.3\times10^{-1}$
	MeOH	70	$6.75\times10^{-3} \pm 3.32\times10^{-8}$	$58.96 \pm 2.68\times10^{-4}$	$1.31\times10^{-2} \pm 3.4\times10^{-3}$	30 ± 8.05	$1.002 \pm 1.7\times10^{-1}$
		95	$6.87\times10^{-3} \pm 1.08\times10^{-7}$	$59.13 \pm 8.54\times10^{-4}$	$1.33\times10^{-2} \pm 3.5\times10^{-3}$	29.98 ± 8.06	$1.002 \pm 1.7\times10^{-1}$
	ACN/MeOH content in the eluent % (v/v)		bi-Langmuir isotherm (M_3)				
			K_1 (L/g)	q_{S1} (g/L_{ads})	K_2(L/g)	q_{S2}(g/L_{ads})	
PH	ACN	70	$8.49\times10^{-4} \pm 3.55\times10^{-9}$	$351.28 \pm 1.34\times10^{-3}$	$7.19 \pm 1.26\times10^{-3}$	$3.59\times10^{-6} \pm 2.64\times10^{-6}$	
		95	$4.46\times10^{-3} \pm 3.22\times10^{-3}$	55.24 ± 108.35	$7.15\times10^{-4} \pm 1.26\times10^{-3}$	462 ± 389.76	
	MeOH	70	$5.46\times10^{-4} \pm 1.72\times10^{-1}$	$760 \pm 5.01\times10^{4}$	$2.15\times10^{-3} \pm 3.2\times10^{-1}$	$140.01 \pm 6.9\times10^{4}$	
		95	$6.7\times10^{-4} \pm 0.102\times10^{-1}$	$300 \pm 1.4\times10^{5}$	$1.8\times10^{-3} \pm 0.66$	$214 \pm 3\times10^{5}$	
CAF	ACN	70	$8.8\times10^{-3} \pm 6.33\times10^{-2}$	28.08 ± 795.23	$3.27\times10^{-3} \pm 0.104$	40.32 ± 326.78	
		95	$9.69\times10^{-3} \pm 6.5\times10^{-1}$	$30 \pm 2.11\times10^{-1}$	$9.83\times10^{-3} \pm 8.45\times10^{-1}$	$30 \pm 1.11\times10^{-1}$	
	MeOH	70	$2.24\times10^{-3} \pm 8.96$	$30 \pm 5.4\times10^{4}$	$1.14\times10^{-2} \pm 2.21$	$30 \pm 1.8\times10^{4}$	
		95	$4.68\times10^{-3} \pm 1.018$	$55 \pm 1.43\times10^{3}$	$1.7\times10^{-2} \pm 2.24$	$9.27 \pm 4.1\times10^{3}$	

Table 3. Statistical analysis: RSS, SD, and Fisher test values for adsorption isotherm models for the Hypersil GOLD HILIC column

	ACN/MeOH content in the eluent % (v/v)		Langmuir isotherm (M_1)		
			RSS	SD	F
PH	ACN	70	9.62×10^{-11}	2.31×10^{-6}	6.42×10^{14}
		95	0.026	3.8×10^{-2}	7.43×10^{6}
	MeOH	70	5.28×10^{-10}	5.41×10^{-6}	6.41×10^{14}
		95	9.55×10^{-10}	7.28×10^{-6}	2.33×10^{14}
CAF	ACN	70	1.1×10^{-3}	7.59×10^{-3}	1.75×10^{6}
		95	1.52×10^{-11}	8.95×10^{-7}	2.82×10^{14}
	MeOH	70	7.42×10^{-12}	6.25×10^{-7}	2.82×10^{14}
		95	8.02×10^{-11}	2.05×10^{-6}	2.71×10^{13}
			Tóth isotherm (M_2)		
PH	ACN	70	1.14×10^{-7}	8.2×10^{-5}	3.4×10^{11}
		95	7.1×10^{-5}	2.04×10^{-3}	1.7×10^{9}
	MeOH	70	7.39×10^{-7}	2.08×10^{-4}	2.88×10^{11}
		95	2.73×10^{-7}	1.26×10^{-4}	5.11×10^{11}
CAF	ACN	70	6.09×10^{-7}	1.84×10^{-4}	1.98×10^{9}
		95	1.8×10^{-3}	9.9×10^{-3}	1.52×10^{6}
	MeOH	70	2.77×10^{-4}	3.92×10^{-3}	4.77×10^{6}
		95	3.05×10^{-4}	4.12×10^{-3}	4.5×10^{6}
			bi-Langmuir isotherm (M_3)		
PH	ACN	70	6.33×10^{-11}	1.99×10^{-6}	4.33×10^{14}
		95	7.32×10^{-4}	6.77×10^{-3}	1.16×10^{8}
	MeOH	70	1.24	2.79×10^{-1}	1.2×10^{5}
		95	2.64	4.06×10^{-1}	3.7×10^{4}
CAF	ACN	70	9.13×10^{-7}	2.32×10^{-4}	9.38×10^{8}
		95	3.65×10^{-2}	4.6×10^{-2}	5.3×10^{4}
	MeOH	70	1.3×10^{-2}	2.7×10^{-2}	7.2×10^{4}
		95	5.5×10^{-3}	1.8×10^{-2}	1.7×10^{5}

data better than the bi-Langmuir model, i.e. the four-parameter bi-Langmuir model is not statistically better than the three-parameter Tóth model. This analysis allows for the assessment of whether the difference in model fit is statistically significant after accounting for the number of parameters in the models.

For CAF, surface heterogeneity was observed in the 70% (v/v) ACN system, as confirmed by the value of the heterogeneity parameter in the Tóth model ($v \approx 0.97$, Table 2). The better fit of heterogeneous models in this system is supported by lower RSS and SD values, as well as higher F-test values compared to the Langmuir model (Table 3). The analysis of the ratio of F-test values (Table 4) clearly indicates that the Tóth model provides the best description of the investigated system. In the remaining systems (95% (v/v) ACN and 70% and 95% (v/v) MeOH), the values of the parameter v are close to unity, indicating the absence of pronounced surface heterogeneity. Under these conditions, the Langmuir model provides an adequate statistical fit, characterized by low RSS and SD values as well as high F-test values. The stability and reliability of the estimated parameters are confirmed by narrow confidence intervals (Table 2), which justifies the application of the Langmuir model. Figures 9 (for PH) and 10 (for CAF) show the obtained adsorption isotherms together with their fits to the most appropriate isotherm model. However, it should be noted that the isotherms exhibit almost linear behavior, which results from the analyzed concentration range corresponding to the initial region of adsorption. In this range,

Table 4. Comparison of the analyzed heterogeneous adsorption isotherm models based on the ratio of Fisher test values for the Hypersil GOLD HILIC column

	ACN/MeOH content in the eluent % (v/v)		bi-Langmuir (M_3) vs Tóth (M_2)		
			$F_{N-16,N-17,\ 5\%}$	$F_{M_3,M_2} = \frac{F_{M_3}}{F_{M_2}}$	$F_{M_3,M_2} \geq F_{N-l_3,N-l_2}$
PH	ACN	95	2.29	0.07	False
	ACN/MeOH content in the eluent % (v/v)		$F_{N-17,N-18,\ 5\%}$	$F_{M_3,M_2} = \frac{F_{M_3}}{F_{M_2}}$	$F_{M_3,M_2} \geq F_{N-l_3,N-l_2}$
CAF	ACN	70	2.23	0.47	False

even nonlinear models, such as the Langmuir, Tóth, and bi-Langmuir models, show behavior close to linear.

For the Shodex SILICA 5NH 4D column, for PH in systems containing 95% (v/v) ACN and 70% (v/v) MeOH, the results confirmed the heterogeneous nature of the stationary phase surface. Statistical analysis (Table 6) showed that the experimental data are best described by heterogeneous models, particularly the bi-Langmuir and Tóth models, which account for variations in binding energy of the analyte to the surface. The RSS, SD, and F-test values indicate a significantly better fit of these models compared to the Langmuir model. Surface heterogeneity is further confirmed by the Tóth model parameter v (Table 5), with values of 0.97 for 95% (v/v) ACN and 0.76 for 70% (v/v) MeOH, indicating deviation from the ideal Langmuir model (v = 1). Additional statistical analysis based on the ratio of F-test values (Table 7) showed that, in the 95% (v/v) ACN system, the Tóth model provides the best fit, whereas in the 70% (v/v) MeOH system, the bi-Langmuir model gives the best description of the data. In the remaining systems, i.e., 70% (v/v) ACN and 95% (v/v) MeOH, the analysis indicated a homogeneous surface character. Consequently, the experimental data are best described by the Langmuir model, as confirmed by statistical parameters and the Tóth model parameter v, which takes values close to unity (1.00 and 1.01, respectively). These results confirm the homogeneous nature of PH adsorption under these chromatographic conditions.

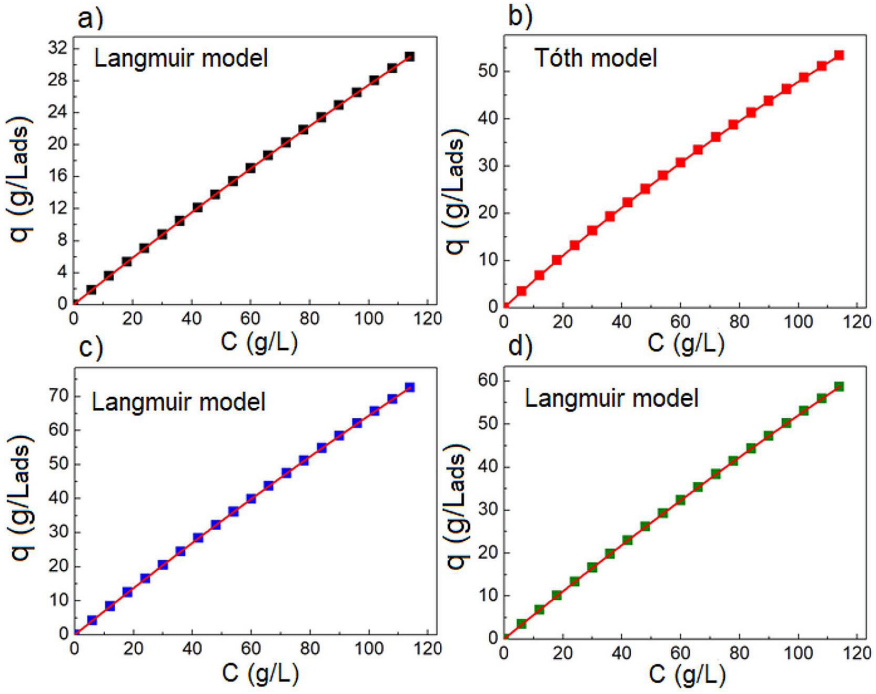

Figure 9. Fitting of the most appropriate adsorption isotherm models to experimental data for PH for the Hypersil GOLD HILIC column in different eluent compositions: a) 70% (v/v) ACN, b) 95% (v/v) ACN, c) 70% (v/v) MeOH, d) 95% (v/v) MeOH

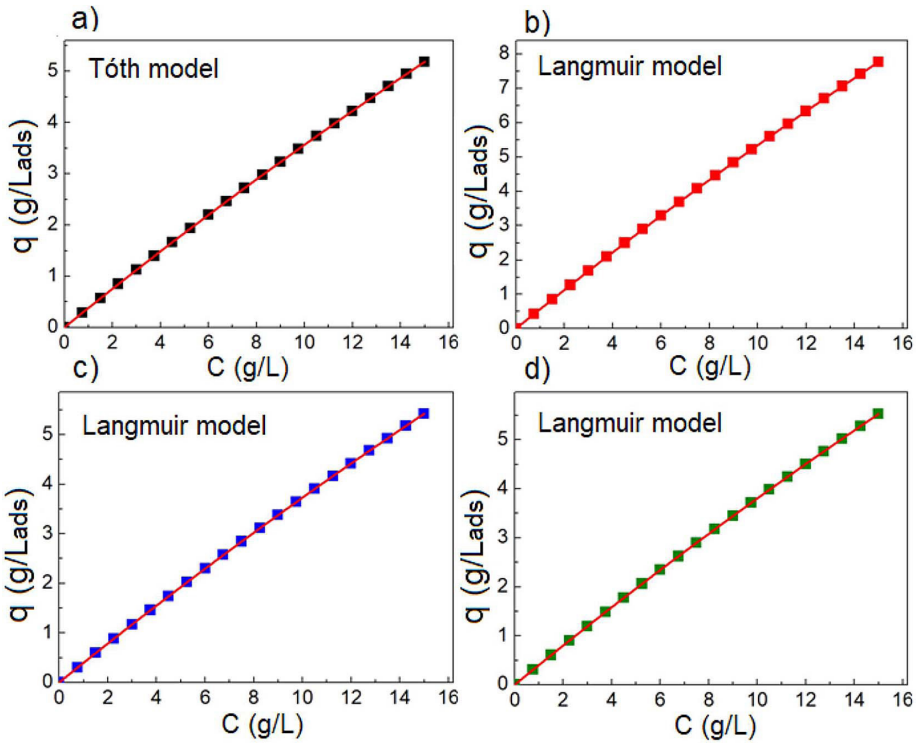

Figure 10. Fitting of the most appropriate adsorption isotherm models to experimental data for CAF for the Hypersil GOLD HILIC column in different eluent compositions: a) 70% (v/v) ACN, b) 95% (v/v) ACN, c) 70% (v/v) MeOH, d) 95% (v/v) MeOH

Table 5. Estimated values of adsorption isotherm model parameters along with confidence intervals for the Shodex SILICA 5NH 4D

	ACN/MeOH content in the eluent % (v/v)		Langmuir isotherm (M_1)		Tóth isotherm (M_2)		
			K (L/g)	q_S (g/L_{ads})	K (L/g)	q_S (g/L_{ads})	v
PH	ACN	70	$8.49\times10^{-4}\pm4.67\times10^{-4}$	$147.57\pm2.8\times10^{-9}$	$4.31\times10^{-3}\pm3.65\times10^{-3}$	28.93±25.48	$1\pm1.58\times10^{-2}$
		95	$1.64\times10^{-3}\pm4.05\times10^{-4}$	400±86.6	$7.89\times10^{-4}\pm3.62\times10^{-5}$	786.61±36.8	$0.97\pm1.56\times10^{-2}$
	MeOH	70	$2\times10^{-3}\pm3.52\times10^{-4}$	205.28±30.99	$1.29\times10^{-4}\pm5.82\times10^{-4}$	$380\pm8.71\times10^{2}$	0.76±0.641
		95	$8.49\times10^{-4}\pm2.88\times10^{-9}$	$494.48\pm1.56\times10^{-3}$	$9.6\times10^{-4}\pm5.92\times10^{-5}$	436±27.42	$1.01\pm2.43\times10^{-2}$
CAF	ACN	70	$1.4\times10^{-2}\pm3.5\times10^{-3}$	30±6.47	$4.91\times10^{-3}\pm9.43\times10^{-4}$	80.63±15.8	$0.87\pm5.5\times10^{-2}$
		95	$9.43\times10^{-3}\pm6.43\times10^{-4}$	123.3±7.6	$2.14\times10^{-3}\pm1.7\times10^{-3}$	570.6±467.4	0.62±0.124
	MeOH	70	$6.75\times10^{-3}\pm3.31\times10^{-8}$	$119.7\pm5.45\times10^{-4}$	$1.6\times10^{-2}\pm4.9\times10^{-3}$	50±15.9	$1.02\pm2.5\times10^{-1}$
		95	$6.75\times10^{-3}\pm3.31\times10^{-8}$	$114.72\pm5.23\times10^{-4}$	$1.89\times10^{-2}\pm6.5\times10^{-3}$	40±14.21	$1.01\pm3.44\times10^{-1}$
	ACN/MeOH content in the eluent % (v/v)		bi-Langmuir isotherm (M_3)				
			K_1 (L/g)	q_{S1} (g/L_{ads})	K_2 (L/g)	q_{S2} (g/L_{ads})	
PH	ACN	70	$5.77\times10^{-4}\pm2.5\times10^{-2}$	$130\pm4.09\times10^{3}$	$1.33\times10^{-3}\pm4.7\times10^{-2}$	$37.99\pm5.8\times10^{3}$	
		95	$3.14\times10^{-4}\pm15.9\times10^{-2}$	$724.75\pm8.82\times10^{3}$	$1.22\times10^{-3}\pm1.1\times10^{-2}$	$321.26\pm10.08\times10^{3}$	
	MeOH	70	$3.46\times10^{-1}\pm8.8\times10^{-5}$	$1.5\pm1.13\times10^{-4}$	$8.8\times10^{-4}\pm5.33\times10^{-7}$	401±0.02	
		95	$5.92\times10^{-4}\pm1.8\times10^{-1}$	$436\pm1.6\times10^{4}$	$2.15\times10^{-3}\pm3.6\times10^{-1}$	$10\pm8.8\times10^{5}$	
CAF	ACN	70	$2.38\times10^{-3}\pm0.42$	$63.62\pm4.02\times10^{3}$	$1.05\times10^{-2}\pm0.32$	$79.92\pm4.5\times10^{4}$	
		95	$6.75\times10^{-3}\pm9.9\times10^{-8}$	$164.08\pm2.05\times10^{-3}$	$8.6\times10^{-1}\pm9.5\times10^{-5}$	$2.5\times10^{-1}\pm1.7\times10^{-5}$	
	MeOH	70	$5.17\times10^{-3}\pm10.12$	$50\pm7.6\times10^{4}$	$1.1\times10^{-2}\pm5.33$	$59.85\pm1.02\times10^{5}$	
		95	$6.98\times10^{-3}\pm51.52$	$57.42\pm2.6\times10^{-6}$	$8.68\times10^{-3}\pm41.54$	$50\pm2.68\times10^{-6}$	

For CAF in the systems containing 70% and 95% (v/v) ACN, pronounced surface heterogeneity of the stationary phase is observed, along with the presence of at least two types of adsorption sites. This is confirmed by the Tóth model parameter v (Table 5), which takes values significantly lower than unity (0.87 and 0.62, respectively), indicating the energetic heterogeneity of adsorption sites. Statistical analysis (RSS, SD, and F-test values; Table 6) showed that under these conditions, heterogeneous models (Tóth and bi-Langmuir) describe the experimental data significantly better than the Langmuir model. Additional comparison of the models based on the ratio of F-test values (Table 7) showed that, for 70% (v/v) ACN, statistically the Tóth model provides the

Table 6. Statistical analysis: RSS, SD, and Fisher test values for adsorption isotherm models for the Shodex SILICA 5NH 4D

	ACN/MeOH content in the eluent, % (v/v)		Langmuir isotherm (M_1)		
			RSS	SD	F
PH	ACN	70	1.7×10^{-11}	9.72×10^{-7}	6.41×10^{14}
		95	6.75	0.61	3.9×10^{4}
	MeOH	70	1.73	3.1×10^{-1}	5.6×10^{4}
		95	1.91×10^{-10}	3.25×10^{-6}	6.41×10^{14}
CAF	ACN	70	6.3×10^{-2}	5.7×10^{-2}	3.2×10^{4}
		95	2.1×10^{-2}	3.3×10^{-2}	81.62×10^{4}
	MeOH	70	3.06×10^{-11}	1.27×10^{-6}	2.82×10^{14}
		95	2.81×10^{-11}	1.22×10^{-6}	2.82×10^{14}
			Tóth isotherm (M_2)		
PH	ACN	70	1.77×10^{-1}	1.02×10^{-1}	3.86×10^{4}
		95	3.57×10^{-4}	4.6×10^{-3}	4.68×10^{8}
	MeOH	70	0.129×10^{-1}	2.75×10^{-1}	4.8×10^{5}
		95	3.65×10^{-4}	4.6×10^{-3}	2.11×10^{8}
CAF	ACN	70	4.32×10^{-5}	1.55×10^{-3}	2.96×10^{7}
		95	4.01×10^{-3}	1.4×10^{-2}	2.66×10^{6}
	MeOH	70	2.2×10^{-3}	1.1×10^{-2}	2.45×10^{6}
		95	3.47×10^{-3}	1.38×10^{-2}	1.44×10^{6}
			bi-Langmuir isotherm (M_3)		
PH	ACN	70	5.68×10^{-5}	1.8×10^{-3}	8.5×10^{7}
		95	4.57×10^{-4}	5.35×10^{-3}	2.58×10^{8}
	MeOH	70	4.43×10^{-9}	1.66×10^{-5}	9.8×10^{12}
		95	4.6×10^{-2}	1.7×10^{-2}	1.2×10^{5}
CAF	ACN	70	9.3×10^{-5}	2.34×10^{-5}	9.73×10^{6}
		95	2.41×10^{-11}	1.19×10^{-6}	3.13×10^{14}
	MeOH	70	4.08×10^{-2}	4.8×10^{-2}	9.4×10^{4}
		95	9.37×10^{-3}	2.34×10^{-2}	3.8×10^{5}

Table 7. Comparison of the analyzed heterogeneous adsorption isotherm models based on the ratio of Fisher test values for the Shodex SILICA 5NH 4D

	ACN/MeOH content in the eluent % (v/v)		bi-Langmuir (M_3) vs Tóth (M_2)		
			$F_{N-16,N-17,\ 5\%}$	$F_{M_3,M_2} = \frac{F_{M_3}}{F_{M_2}}$	$F_{M_3,M_2} \geq F_{N-l_3,N-l_2}$
PH	ACN	95	2.29	0.55	False
	MeOH	70	2.29	2.04×10^{4}	True
	ACN/MeOH content in the eluent % (v/v)		$F_{N-17,N-18,\ 5\%}$	$F_{M_3,M_2} = \frac{F_{M_3}}{F_{M_2}}$	$F_{M_3,M_2} \geq F_{N-l_3,N-l_2}$
CAF	ACN	70	2.23	0.33	False
	ACN	95	2.23	1.2×10^{8}	True

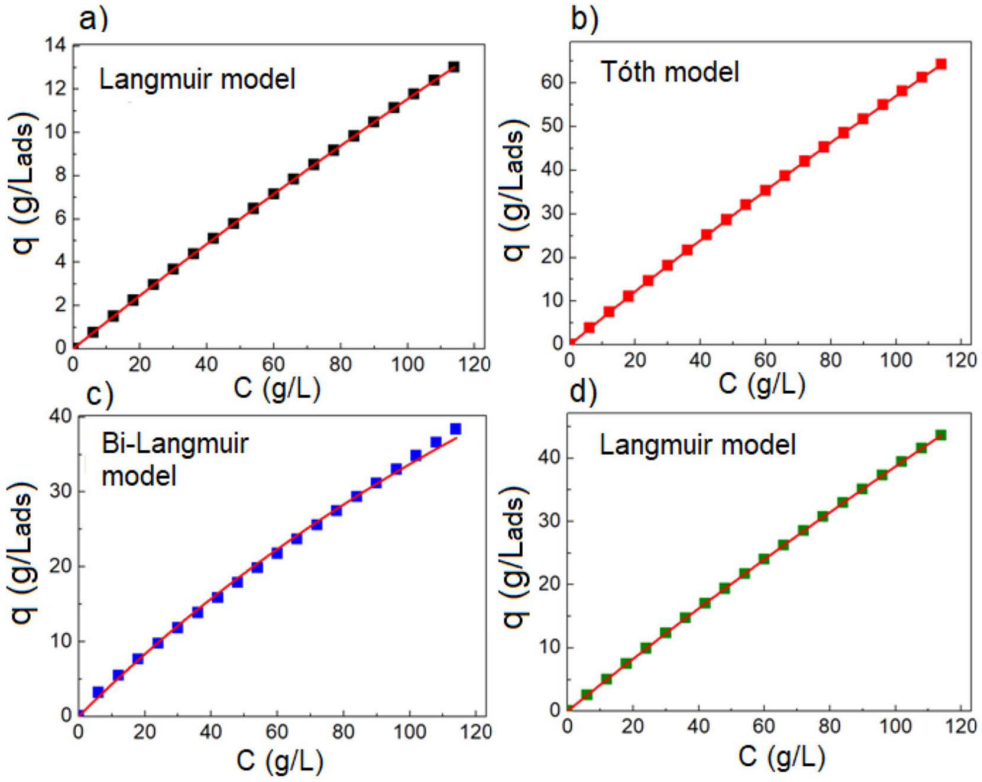

Figure 11. Fitting of the most appropriate adsorption isotherm models to experimental data for PH for the Shodex SILICA 5NH 4D column in different eluent compositions: a) 70% (v/v) ACN, b) 95% (v/v) ACN, c) 70% (v/v) MeOH, d) 95% (v/v) MeOH

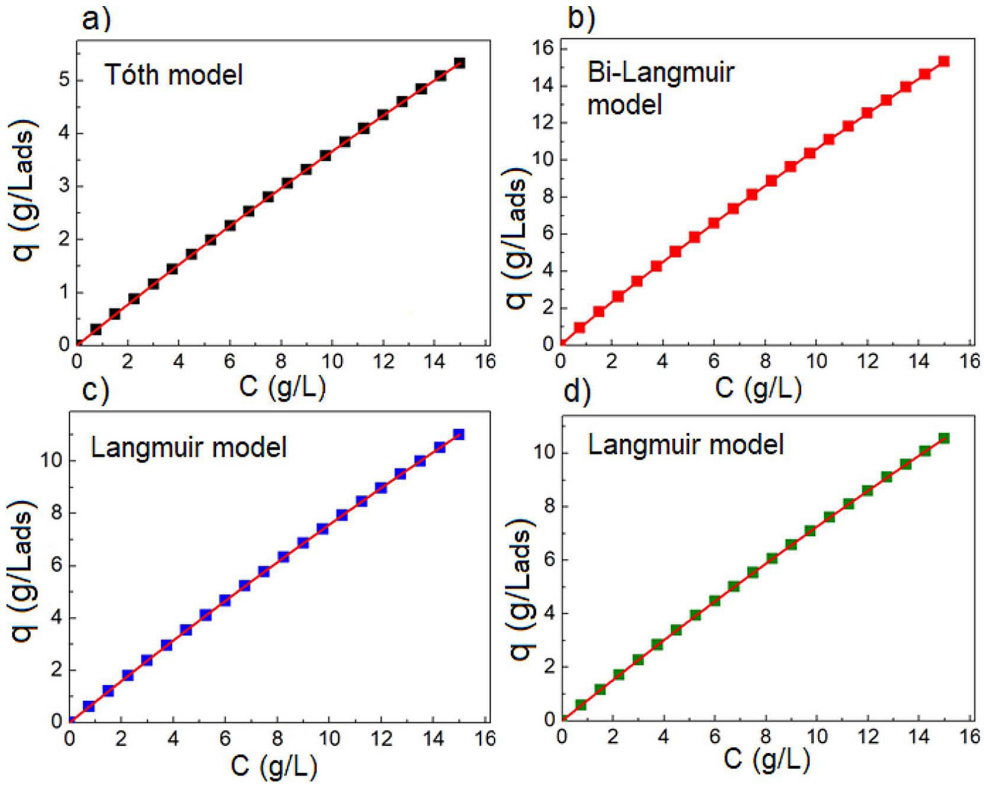

Figure 12. Fitting of the most appropriate adsorption isotherm models to experimental data for CAF for the Shodex SILICA 5NH 4D column in different eluent compositions: a) 70% (v/v) ACN, b) 95% (v/v) ACN, c) 70% (v/v) MeOH, d) 95% (v/v) MeOH

best fit, whereas for 95% (v/v) ACN, the bi-Langmuir model provides the best statistical description of the data. In contrast to the acetonitrile-based systems, in the systems containing 70% and 95% (v/v) MeOH, CAF adsorption exhibits characteristics of a homogeneous surface. Under these conditions, statistical analysis clearly indicates that the Langmuir model provides the best fit compared to heterogeneous models. Figure 11(for PH) and Figure 12 (for CAF) present the obtained adsorption isotherms together with their fits to the most appropriate isotherm model.

CONCLUSIONS

The obtained results clearly demonstrate that the availability of energetic sites and the nature of surface heterogeneity depend on the type of stationary phase, the composition of the mobile phase, and the physicochemical properties of the analytes. In the investigated systems, low-energy sites predominate. However, under specific conditions, a significant contribution of high-energy sites is also observed, indicating the heterogeneous nature of stationary phase surfaces applied in the HILIC chromatography. It was shown that the appropriate selection of an adsorption isotherm model should directly reflect the energetic characteristics of the surface. For systems exhibiting homogeneous behavior, the Langmuir model provides an adequate description of the experimental data. In contrast, for heterogeneous systems, significantly better fits are obtained using the models that account for surface energy heterogeneity, such as the Tóth and bi-Langmuir models. Statistical analysis confirmed that incorporating surface heterogeneity is essential for the correct interpretation of adsorption data. The applied integrated approach, combining adsorption energy distribution analysis, Scatchard plots, and adsorption isotherm modeling, enables not only quantitative characterization of the adsorption process, but also its physicochemical interpretation. The results indicate that surface heterogeneity is not an constant property but depends on chromatographic conditions, particularly the composition of the mobile phase, the nature of the analyte and the type of stationary phase The study also demonstrated that the changes in eluent composition influence the degree of analyte solvation and the availability of active sites on the stationary phase surface, which directly affects the retention mechanism and the efficiency of the separation process.

Overall, the obtained results contribute to a deeper understanding of adsorption mechanisms in HILIC/RP systems and provide a basis for a more informed selection of adsorption isotherm models in the analysis of chromatographic data. Consequently, they may support the development and optimization of chromatographic methods, especially for the separation of compounds with diverse physicochemical properties.

Acknowledgments

Financed by the Minister of Science and Higher Education Republic of Poland within the program “Regional Excellence Initiative”, agreement no. RID/SP/0032/2024/01.

REFERENCES

1. Valášek J., Hekerle L., Nechvátalová M., Bednařík A., Preisler J., Urban J. Effect of stationary phase surface chemistry and particle architecture in proteomics, J. Chromatogr. A, 2025; 1752:465976, https://doi.org/10.1016/j.chroma.2025.465976
2. Haseeb A., Wondmagegne Y., Fernandes M.X., Samuelsson J. Adsorption energy distributions: Theory and applications in liquid chromatography, J. Chromatogr. Open, 2025; 8:100252, https://doi.org/10.1016/j.jcoa.2025.100252
3. Lech-Przywara R., Galek T., Przywara M., Zapała L., Zapała W. Structural and surface characterization of adsorbents applied in liquid chromatography, Adv. Sci. Technol. Res. J., 2025; 19(9):292–309, https://doi.org/10.12913/22998624/207426
4. Dembek M., Bacskay I., Buratti A., Catani M., Felinger A., Buszewski B., Bocian S. Retention mechanism on phosphodiester stationary phases in hydrophilic interaction liquid chromatography and purely aqueous mobile phase part II: Overloading with limited soluble samples, J. Chromatogr. A, 2024; 1715:464596, https://doi.org/10.1016/j.chroma.2023.464596
5. Ng K., Burhan M., Shahzad M., Ismail A. Universal isotherm model to capture adsorption uptake and energy distribution of porous heterogeneous surface, Sci. Rep., 2017; 7, https://doi.org/10.1038/s41598-017-11156-6
6. McCalley D.V. Influence of metals in the column or instrument on performance in hydrophilic interaction liquid chromatography, J. Chromatogr.

A, 2022; 1663:462751, https://doi.org/10.1016/j.chroma.2021.462751

7. Haseeb A., Wondmagegne Y., Fernandes M.X., Samuelsson J., Introducing the adsorption energy distribution calculation for two component competitive adsorption isotherm data, Anal. Chem., 2025; 97:1966−1971, https://doi.org/10.1021/acs.analchem.4c04663
8. Bocian S., Buszewski B. Residual silanols at reversed-phase silica in HPLC – a contribution for a better understanding, J. Sep. Sci., 2012; 35(10–11):1191–1200, https://doi.org/10.1002/jssc.201200055
9. Ÿsberg D., Samuelsson J., Fornstedt T. A fundamental study of the impact of pressure on the adsorption mechanism in reversed-phase liquid chromatography, J. Chromatogr. A, 2016; 1457:97–106, https://doi.org/10.1016/j.chroma.2016.06.036
10. Tsui H.W., Lin S.Z., Hsu Y.C., Dai F.J. Retention modeling and adsorption mechanisms in reversed-phase liquid chromatography, J. Chromatogr. A, 2022; 1662:462736, https://doi.org/10.1016/j.chroma.2021.462736
11. Aasim M., Kakarla P.B., D'Souza R.N., Bibi N.S., Klein T.Y., Treccani L., Rezwan K., Fernández-Lahore M. The role of ligands on protein retention in adsorption chromatography: A surface energetics approach, J. Sep. Sci. 2014; 37:618–624, https://doi.org/10.1002/jssc.201301338
12. Gorshenin A., Kazakov I., Korolev V. On the convergence of median versions of the expectation-maximization algorithm for the separation of finite normal mixtures, J. Math. Sci., 2022; 267:92–98, https://doi.org/10.1007/s10958-022-06109-y
13. Matsumura T., Nagamura N., Akaho S., Nagata K., Ando Y. Spectrum adapted expectation-maximization algorithm for high-throughput peak shift analysis, Sci. Technol. Adv. Mater., 2019; 20:733–745, https://doi.org/10.1080/14686996.2019.1620123
14. Lech-Przywara R., Przywara M., Bukowska A., Galek T., Zapała W. Brief analysis of selected sorption and physicochemical properties of three different silica-based adsorbents, Biomed J. Sci. Tech. Res., 2023; 51(2):42478–42485. https://dx.doi.org/10.26717/BJSTR.2023.51.008068
15. Jandera P., Janás P. Recent advances in stationary phases and understanding of retention in hydrophilic interaction chromatography. A review, Anal. Chim. Acta, 2017; 967:12–32, https://doi.org/10.1016/j.aca.2017.01.060
16. Guo Y., Baran D. Hydrophilic partitioning or surface adsorption? a quantitative assessment of retention mechanisms for hydrophilic interaction chromatography (HILIC), Molecules, 2023; 28, https://doi.org/10.3390/molecules28186459
17. Ziobrowski P., Chutkowski M., Przywara M., Zapała L., Kosińska-Pezda M., Zapała W. Analysis of adsorption energy distribution in selected hydrophilic-interaction chromatography systems with amide, amine and zwitterionic stationary phases. J. Sep. Sci., 2021, https://doi.org/10.1002/jssc.202100160
18. Lech-Przywara R., Zapała W. Analysis of selected factors influencing the course of the process in liquid chromatography, Adv. Sci. Technol. Res. J., 2025; 19(6):1–16. https://doi.org/10.12913/22998624/202507
19. Wang J., Guo X. Adsorption isotherm models: Classification, physical meaning, application and solving method, Chemosphere, 2020; 258:127279, https://doi.org/10.1016/j.chemosphere.2020.127279
20. Ayawei N., Ebelegi A., Wankasi D. Modelling and interpretation of adsorption isotherms. J. Chem., 2017; 1–11, https://doi.org/10.1155/2017/3039817
21. Zhang J., Bai J., Duan M., Yang J., Bian L. Derivation of adsorption capacity and adsorption isotherm by a single adsorbate concentration in liquid–solid system, Chem. Pap., 2021; 75:2459–2476, https://doi.org/10.1007/s11696-020-01476-9
22. Morbidelli M. Introduction to "Fundamentals of Preparative and Nonlinear Chromatography" by G. Guiochon, A. Felinger, D.G. Shirazi [Elsevier, Amsterdam, 2nd ed., 2006, Ch. 1], J. Chromatogr. A, 2016; 1446:10, https://doi.org/10.1016/j.chroma.2016.03.050
23. Gritti F., Tarafder A., Guiochon G. Interpretation of dynamic frontal analysis data in solid/supercritical fluid adsorption systems. I: Theory, J. Chromatogr. A, 2013; 1290:73–81, https://doi.org/10.1016/j.chroma.2013.02.049
24. Jandera P., Hájek, T. A New Definition of the stationary phase volume in mixed-mode chromatographic columns in hydrophilic liquid chromatography, Molecules, 2021; 26:4819, https://doi.org/10.3390/molecules26164819
25. Liu Q., OuYang L., Liang H., Li N., Geng X. A novel thermodynamic state recursion method for description of nonideal nonlinear chromatographic process of frontal analysis. J. Sep. Sci., 2012; 35:1411–1423, https://doi.org/10.1002/jssc.201200018
26. Kamińska J., Zapała W., Influence of modifier concentration on retention in hydrophilic interaction chromatography – preliminary study, Inż. Ap. Chem., 2015; 54(1):4–7 (in Polish).
27. Zhang J., Yang, Y., Ding J., Information criteria for model selection, WIREs Comput. Stat., 2023; 15(5):607, https://doi.org/10.1002/wics.1607